Journal of Coastal Research	13	2	349–362	Fort Lauderdale, Florida	Spring 1997

Response of a Small-Scale Bottom-Attached Estuarine Plume to Wind and Tidal Dissipation

Jackson O. Blanton†, Julie Amft† and Tom Tisue‡

†Skidaway Institute of Oceanography
10 Ocean Science Circle
Savannah, GA 31411, U.S.A.

‡Department of Chemistry
Clemson University
223 Chemistry Building
Clemson, SC 29634, U.S.A.

ABSTRACT

BLANTON, J.O.; AMFT, J., and TISUE, T., 1997. Response of a small-scale bottom-attached estuarine plume to wind and tidal dissipation. *Journal of Coastal Research,* 13(2), 349–362. Fort Lauderdale (Florida), ISSN 0749-0208.

Ebb tide advects low salinity discharges onto the continental shelf where they mix with ambient shelf water. Only a portion of the mixture returns on the flood tide into the estuary. The remainder often forms a low salinity zone detached from the parent estuarine plume. Shipboard and aerial surveys conducted in autumn were used to determine the fate of the estuarine discharge from Charleston Harbor, South Carolina. We used a simple momentum balance to estimate the wind generated alongshelf current. We found that the plume deflection was predicted by the vector addition of the wind generated current and the tidal current operating at the observation times. Thus, the plume is easily deflected downwind since wind stress in shallow water is transferred directly to the bottom. A sequence of cross-plume sections was obtained during a portion of the ebb and flood tidal cycle. Ebb flow carried low salinity estuarine water seaward where it turned abruptly southward as it encountered the southward current that prevails along the shelf in autumn. The front separating estuarine discharge from shelf water was significantly stronger on the upstream side than it was on the downstream side, as indicated by salinity and suspended matter content that sharply distinguished the two water masses. During the flood stage, the upstream front weakened significantly.

ADDITIONAL INDEX WORDS: *Energy balance, tidal currents, mixing.*

INTRODUCTION

The interaction of estuarine plumes with the ocean has implications for pollution, larval transport and sediment transport. The gravitational circulation in the estuary may extend onto the shelf (PAPE and GARVINE, 1982; GARVINE, 1991) so that material near the bottom is transported into the estuary. Low salinity estuarine discharges can form a buoyancy-driven coastal current on inner continental shelves. In the deep shelf waters off Norway and Alaska, the current flows in a shallow upper layer decoupled from the bottom (MORK, 1981; ROYER, 1981; JOHANNESSEN *et al.*, 1989). On the other hand, coastal currents connected to estuarine discharges on shallow shelves have prolonged contact with the bottom (BLANTON, 1981; HEARN *et al.*, 1985; SIMPSON and HILL, 1986; GARVINE, 1991). These interactions offer efficient pathways for the transport of material back and forth between estuary and ocean. MASSE (1990) and GARVINE (1991) have comprehensive literature reviews of theoretical and observational studies focused on estuarine/ocean coupling.

This paper describes the configuration of the estuarine plume emanating from Charleston Harbor (Figure 1) during different phases of the tidal cycle. Data from this study consist of several horizontal and vertical sections of the plume. The dissipation of the upstream edge of the plume (hereafter called the Charleston Plume) is also described. This edge is defined by a sharp change in color as estuarine water encounters coastal shelf water flowing southward into the plume, designated hereafter as the "upstream" edge.

We begin the paper with a description of the Charleston Plume as revealed by aerial photographs. A sequence of photos together with hydrographic data obtained during different stages of the tide are used to show how the plume jets seaward onto the shelf during low tide and switches onshore and to the south during flood tide.

The main purpose of this paper is to show that (1) the Charleston Plume is typical of bottom-attached plumes and that it is easily deflected by alongshelf currents, and (2) the stratification in the plume supported by buoyancy advection is closely balanced by the tendency of tidal power to dissipate the plume. We display details of the cross-plume density structure and its temporal evolution from two hours before slack ebb flow until two hours after slack ebb (flood) flow. Changes in potential energy are then used to quantify the dissipation processes as the pressure due to the convergence along the upstream edge of the front decreases.

BACKGROUND

Mixing Processes in Shelf Water

The inlet through which the Charleston Plume exits is like one of the many inlets that connect low-lying coastal marshes to the ocean in the southeastern U.S. Low salinity discharges through these inlets form plumes of low salinity, low density water near the coast. Subsequent tidal and wind mixing blends these plumes into a band of low salinity water that

95063 received 17 July 1995; accepted in revision 20 August 1995.

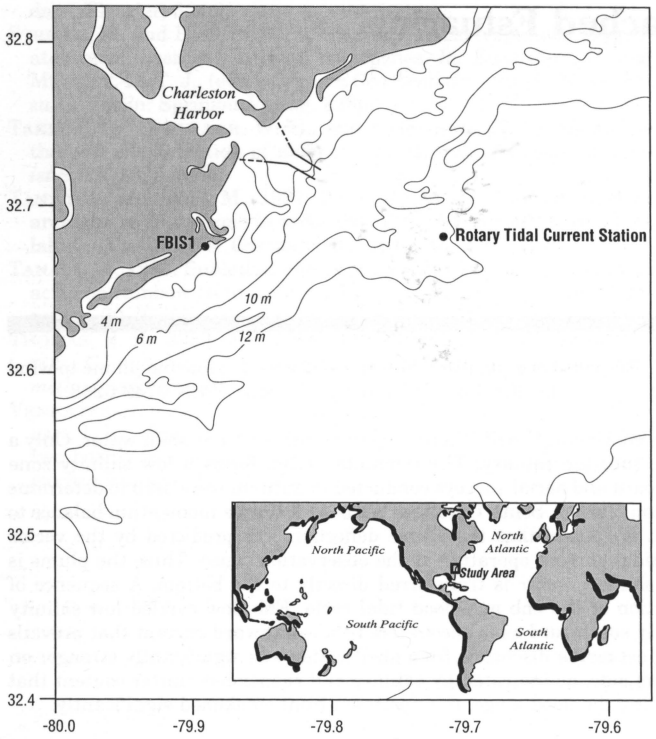

Figure 1. Location map of the Charleston Harbor plume study. Locations of FBIS1 and rotary tidal current station are shown. Bold lines at mouth of harbor denote jetties (partially submerged at the shore) between which a 13-m deep channel is maintained.

extends along the coast over a distance greater than 400 km. This band represents the accumulated effect of many of the other rivers that similarly discharge water to the continental shelf.

Tidal power provides an efficient and ever-present energy source that mixes the low salinity discharges along the coast. BLANTON and ATKINSON (1983) estimated that tidal power dissipated at the bottom ranges from 0.3×10^{-4} to 2×10^{-4} W m^{-2} off the Georgia coast. This is sufficient to mix vertically the buoyancy resulting from heating. Except in localized shoal areas adjacent to the coast, this power is too weak to mix vertically the buoyancy provided by even normal discharge of fresh water. At times of peak fresh water discharge, stratification may extend to the mid-shelf (BLANTON, 1995, *unpublished*).

Wind stress can provide a significant increment of power over that generated by tidal currents (VAN AKEN, 1986). Mixing power from strong wind events can range from 1×10^{-3} to 3×10^{-3} W m^{-2} (ATKINSON and BLANTON, 1986), an order of magnitude greater than that provided by tidal power. Thus, the extent of fully mixed coastal waters varies with weather events. Whether complete mixing actually occurs depends primarily on the direction and strength of alongshore winds (BLANTON *et al.*, 1989b). Southward alongshore stress efficiently mixes the water vertically by advecting dense water from offshore into the coastal front, leading to convective instability and vertical mixing. The frontal zone is then characterized primarily by horizontal density gradients. Northward stress, on the other hand, advects low density water offshore and produces a frontal zone with strong vertical density gradients and relatively small horizontal gradients. This dramatic change in frontal structure can occur within a day or less of an alongshore wind stress reversal (BLANTON *et al.*, 1989b).

Plume Dynamics

Plumes formed by estuarine discharges during ebb tide form sharp fronts with ambient shelf water. Within the plumes themselves, the buoyancy flux during ebb tide is sufficient to prevent the mixing power of winds and tidal currents from destroying them. Nearshore, the plume is intense and quite shallow. Farther offshore, the plume generally deepens due mainly to the progressive downward mixing provided by the cross-front circulation as parcels of water are carried offshore and along the front (GARVINE and MONK, 1974; IMBERGER, 1983). The downward mass flux is supplied by horizontal inflow of brackish water from more remote regions of the plume. In the offshore portions of the plume, an upward migration of all isopycnals is observed with an increase in cross-front density gradient and in surface color contrast.

Estuarine plumes in shallow water often form a bottom-attached jet during the initial stages, which then lifts off at a depth proportional to the square root of the jet speed (HEARN *et al.*, 1985; SAFAIE, 1978). Weaker jets corresponding to smaller tidal falls or lower run-off, lift off closer to the discharge point. Bottom friction produced by mass entrainment and lateral inflow into the jet weakens the buoyancy force tending to lift the plume upward. Compared to unattached plumes, the effects of mass entrainment through the entire plume boundary are smaller for bottom-attached jets.

Plumes entering alongshelf flow are turned downstream and may ultimately become attached to shore (JIRKA *et al.*, 1981; HEARN *et al.*, 1985; GARVINE, 1987). The turning is due to the blocking of the alongshelf flow by the bottom-attached jet, resulting in the build-up of a pressure differential across the jet which yields an alongshelf acceleration and an *onshore* Coriolis reaction. As a result, the jet loses all its offshore momentum and becomes attached to the coastline. The attachment width (distance jet penetrates onto shelf) increases as the jet discharge increases and the speed of the coastal current decreases. Large eddies are often formed on the shore side of the plumes jetting into alongshelf flow on the shelf (SAFAIE, 1978; HEARN *et al.*, 1985; MASSE and MURTHY, 1990).

Many of these features are probably present in the Charleston Plume and have been observed in the Niagara Plume (MASSE and MURTHY, 1990, 1992). Such plumes appear to form two regions in the northern hemisphere: (1) a turning region where water is deflected to the right by Coriolis force followed by (2) a coastal current bounded on the right by the coast (looking downstream) where the momentum balance is primarily geostrophic. Recirculating eddies (anticyclonic) are sometimes observed over Niagara Bar probably analogous to

eddies observed in hydraulic models. (SAFAIE, 1978). MASSE and MURTHY (1992) showed that the plume executes an anticyclonic turn 53% of the time and goes directly offshore 26% of the time. Near the river mouth, the plume is vertically mixed to the bottom and the large initial flow deceleration is balanced by bottom stress; away from river mouth, the balance is between Coriolis force, relative acceleration (inertial turning) and the cross-stream baroclinic pressure gradient.

FIELD METHODS

Two surveys of the Charleston Plume were conducted in the autumn during 1990 and 1991. The 1991 survey measured the horizontal configuration of the plume during three stages of the tide. The configuration was defined in terms of suspended solids and salinity at the surface.

The 1990 survey was targeted to define the changes in salinity, density and beam attenuation along the abrupt discontinuity of the plume as it encountered continental shelf water. This survey gave information on the dissipation of the strong front, separating the plume from ambient shelf water as ebb currents ceased and flood currents began.

The ships used for both experiments were each equipped with a CTD instrument which recorded vertical profiles of conductivity (C), temperature (T), beam attenuation and depth (D). Salinity and density were calculated from the conductivity, temperature and depth values using standard algorithms. The CTD unit was lowered through the water column and real-time data displayed on a personal computer; the vertical structure of the water column could immediately be ascertained. Data from each CTD downcast were averaged by depth into 1.0-m bins. The bin-averaged data were then grouped appropriately to create contour plots of selected parameters.

Plume Survey of 1990

The NOAA Ship, FERREL, and the Skidaway Institute of Oceanography Research Vessel, BLUE FIN, carried out several hydrographic surveys in October 1990. A Sea-Bird Electronics, Inc. CTD was used on the FERREL and an Inter-Ocean Systems Inc. S4 CTD was used on the R/V BLUE FIN. An optional SEA TECH beam transmissometer was installed on each CTD unit to measure vertical profiles of suspended particle concentration in the water column. The transmissometer data were not calibrated with suspended sediment samples, so they only represent relative turbidity values. Beam attenuation coefficients were used instead of percent transmission because the transmissometer on the FERREL had a pathlength of 5 cm and the BLUE FIN transmissometer had a pathlength of 10 cm.

Plume Survey of 1991

The NOAA Ship FERREL was used in the plume survey of 1991. This ship had a Sea-Bird Model 19 CTD which was used to collect vertical profiles of salinity and temperature at selected stations. Increased spatial resolution was made possible using a smaller launch equipped with a Solomat 2000 salinity-temperature meter. Sampling was conducted along a predetermined sampling grid in order to define the configuration of the plume as it entered shelf water. Each survey was conducted over an interval of 2 to 2.5 hr centered at slack low water (16 Nov), maximum ebb currents (17 Nov) and maximum flood currents (18 Nov).

At each CTD station, total suspended solids (TSM) were determined for water samples taken 1 m below the surface and 1 m above the bottom. TSM values were based on the U.S. Environmental Protection Agency (USEPA) procedure for non-filterable residue (USEPA, 1979), except that pressure (40 psig) was used rather than vacuum filtration following BAILEY (1988). Our experience has shown that his method is reproducible to within a few percent for the 4-litre sample volumes of inner shelf waters.

RESULTS

Plume Surveys

Three surveys (Figures 2–4) were conducted at times of maximum ebb tidal currents, low water, and maximum flood tidal currents. For each of these conditions, we show a surface salinity map superimposed on the surface TSM field. A 1-km grid is used to reference the locations of stations. Straight lines on the surface map indicate where vertical cross-sections of salinity are displayed.

During maximum ebb, the plume was bent southward (Figure 2). The core of lowest surface salinity was displaced shoreward about 1 km relative to the maximum total concentration of TSM. An oblique section closest to the outlet at the jetties showed highest salinity located in the deep channel leading into the harbor. Above the deep channel, near surface salinities were lowest to the southwest of the flow exiting the harbor. Farther offshore, the southwestward displacement of low salinity surface water is clear. The section did not go far enough shoreward to determine the width of the plume. The core of the TSM maximum was situated in the surface salinity front. The section farthest from shore showed a plume about 5 m deep overriding shelf water of ambient salinity above 34 psu. The maximum surface TSM appeared to fill the low salinity core at the surface. There is no clear indication that the plume was separated from the bottom, but neither was it clearly attached.

Vertical section 'D' (Figure 2) slices obliquely across the axis of the plume. The southernmost station in this section is outside the plume and helps define the surface plume front farther offshore. Here we see evidence that the plume has separated from the bottom where depths are greater than 7 m. The shape of the frontal zone at the base of the plume appeared to follow the bottom depth profile.

The plume at low slack water (Figure 3) was defined by a low salinity core at the entrance to the jetties. There is no obvious deflection of the plume. However, there are two salinity fronts at the south end of the jetties that define a high salinity patch with lower salinity on the shoreward side of the patch. The water was too shallow to obtain data closer to shore. A vertical section shows a plume of cold low salinity water being discharged at the mouth through a slightly warmer and saltier core. The cold fresh core is correlated with maximum TSM concentrations at the mouth and represents

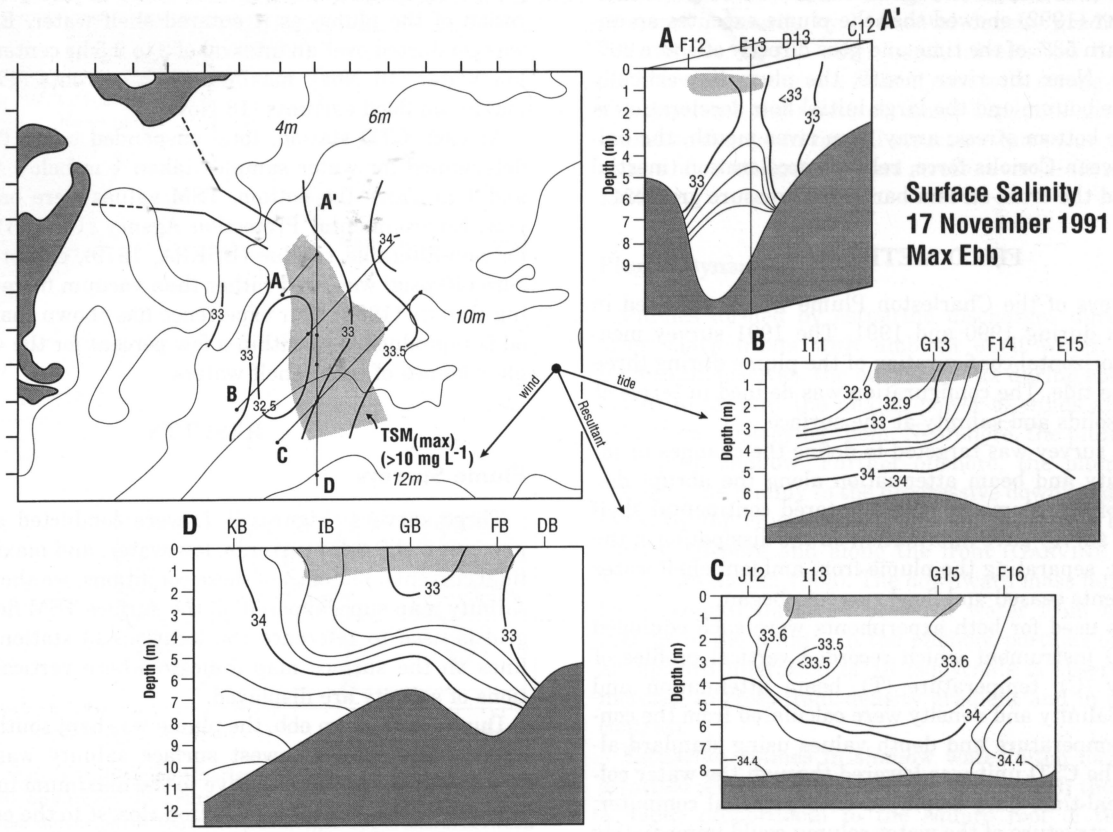

Figure 2. Survey during maximum ebb tide on 17 November 1991. (a) surface salinity map with zone of maximum TSM shaded; (b)–(d) vertical salinity sections.

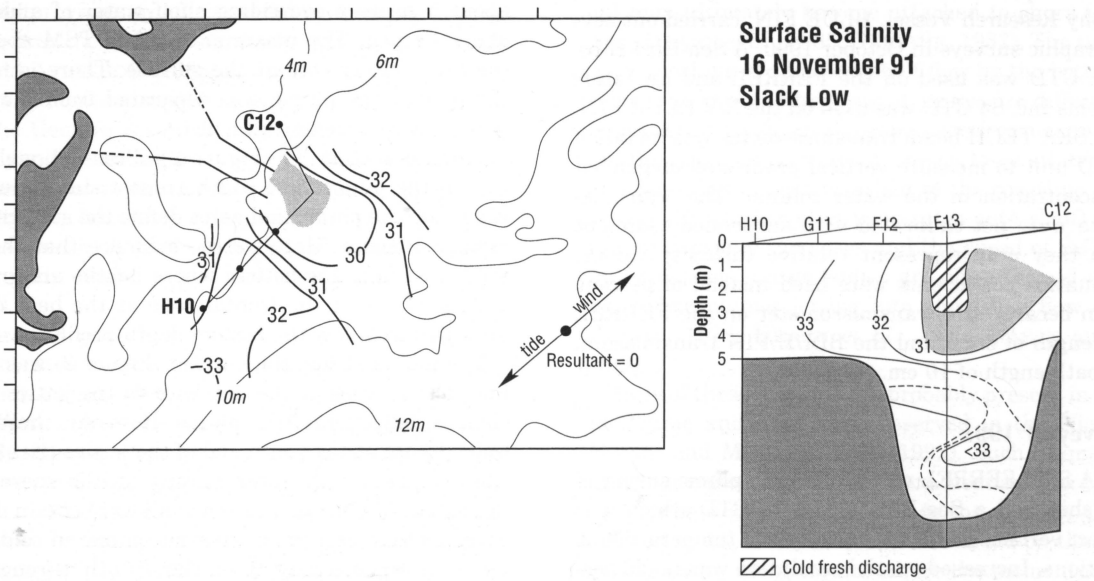

Figure 3. Survey during low water on 16 November 1991 showing surface and vertical salinity distribution with zone of maximum TSM (shaded).

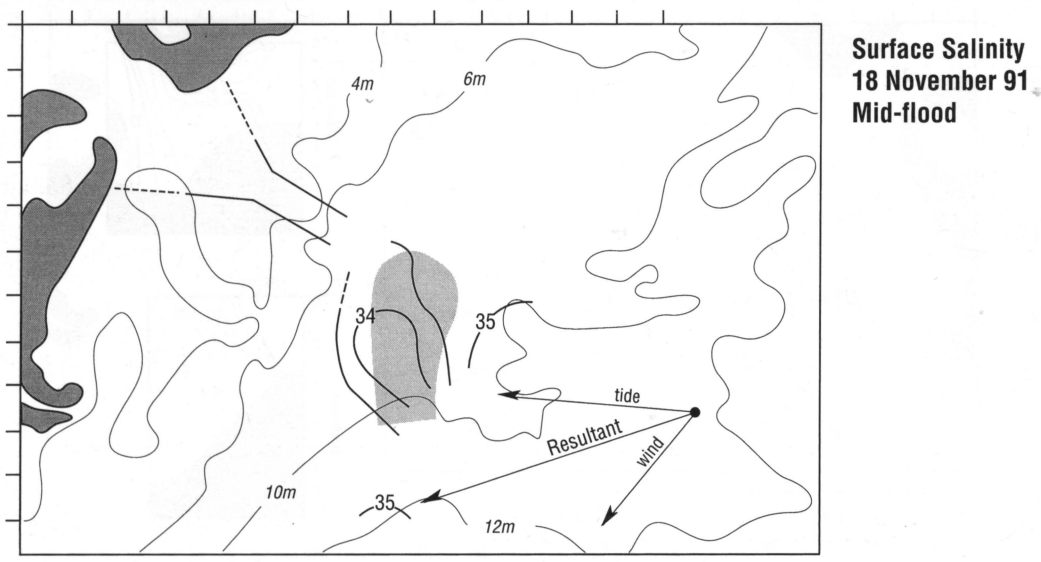

Figure 4. Survey during mid flood tide on 18 November 1991 showing surface salinity map with zone of maximum TSM.

the outflow of estuarine water forced by the freshwater discharge during slack water.

The plume during maximum flood (Figure 4) shows an ill-defined patch of low salinity water south of the jetties. The plume was bent slightly southward, and the zone of TSM did not clearly coincide with the lowest surface salinities. The lowest salinity water was "severed" from the inflowing water through the cut and showed no indication of reentering the harbor.

In summary, surface TSM concentrations showed good correlations with lowest salinities. On the ebb and flood surveys, the maximum TSM concentrations were located on the upstream side of the surface salinity minimum.

A low and high tide survey were conducted on 30 October 1990. This was followed one day later by a survey which began at maximum ebb flow and continued through low slack water and ended 2 hr after flood flow began.

The plume at low tide was bent dramatically southward (Figure 5). The low salinity core was presumably closer to shore in water too shallow for us to operate the boats. Vertical sections show a shallow plume about 2 or 3 m deep just south of the jetty mouth. There was no indication of the plume 1 km seaward. The section cutting across the front showed the offshore extremity but we were unable to define the inshore edge. At high tide (Figure 6), there was no surface expression of the plume near the mouth. Rather, a section across the mouth revealed a high salinity region with lower salinity on either side. The frontal zone was stronger on the nearshore side and extended to the bottom.

The following day, a survey was done at maximum ebb flow. This survey revealed a plume extending offshore and bent southward (Figure 7). The plume front was stronger on the south side. Nevertheless, the front on the northern side had a distinct surface expression easily visible from the boat. We selected that front for a more detailed study of the changes in properties across the front as the maximum ebb flow decreased and the front dissipated.

Dissipation of Plume

The R/V BLUE FIN conducted a detailed survey of the northern side of the plume (Figure 8). Two short transects were done close to the jetties followed by a series of station pairs on either side of a visible turbidity front. The surface front was so sharp that the bow of our 23-m research vessel could be placed on one side of the front and the stern on the other. The station separation of each profile pair was usually less than 100 m, but the exact spacing was within the error of the LORAN positioning system that we used. Conditions were calm and wind did not affect the ship's position. The ship was carried offshore then onshore by the tidal current as we followed the surface demarcation of the plume (Figure 8). The station pairs began during ebb flow, about 2 hr before slack water, and continued almost 2 hr into flood. The location of the plume edge over this time interval (Figure 8) indicated that the plume bent southward then drifted closer to shore during the flood phase of the tide. The predicted tidal ellipse for this phase of the study is superposed on the map (Figure 8).

The northern edge of the plume was defined by two transverse sections (Figure 9) obtained during ebb flow and taken 40 min apart. The first consisted of three hydrographic stations each separated by 350 m about 2 km off the jetties (Figure 9a). The first station was obviously in the surface expression of the turbid water emanating from the mouth of the jetties while the third station was in noticeably clearer waters. There were several surface fronts visible between the stations. The second section had two stations separated by 650 m about 4 km off the jetties (Figure 9b). Both sections showed a frontal zone with isopycnals sloping upward into

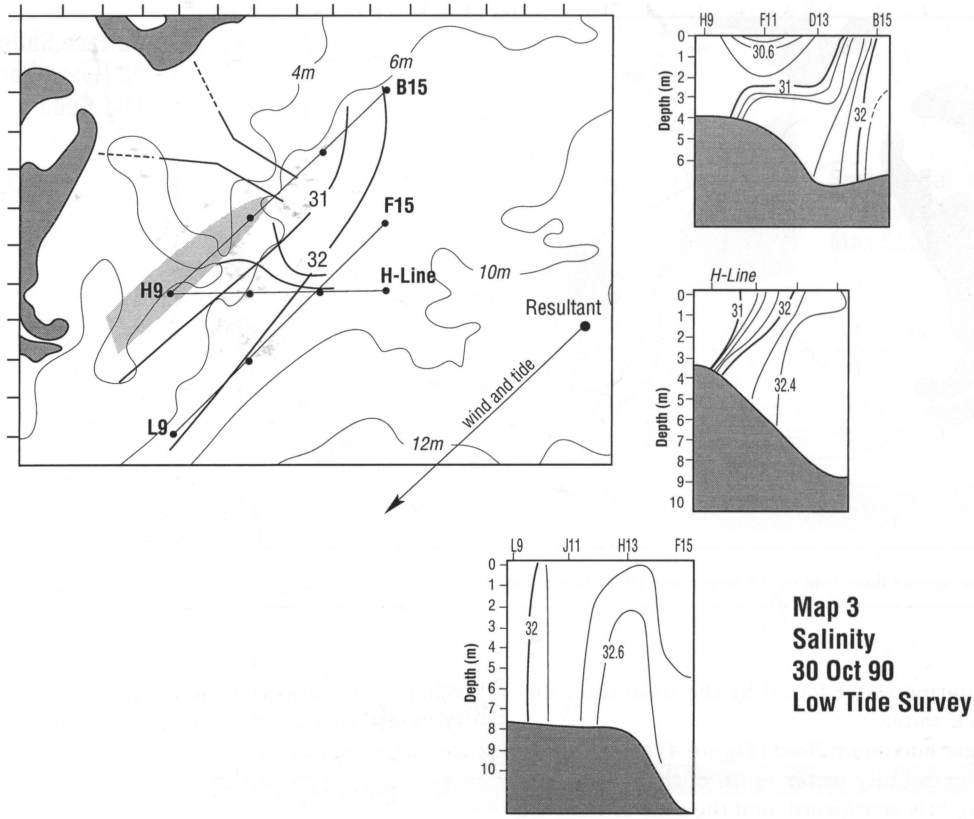

Figure 5. Survey during low water on 30 October 1990 showing surface salinity (zone of maximum TSM shaded) and vertical salinity sections.

ambient shelf water. The vertical density gradient ($\sim 2 \times 10^{-2}$ kg m^{-4}) was slightly greater in the first section closest to the mouth, and the horizontal gradient ($\sim 1 \times 10^{-3}$ kg m^{-4}) was greater in the second section. The compact nature of the front and its steep slope is demonstrated by the fact that the vertical density gradient was only 20 times greater than the horizontal gradient.

Vertical Profiles of Salinity and Beam Attenuation

We measured changes in water properties on either side of the visible front by obtaining pairs of CTD profiles, one in green shelf water and the other in brown turbid estuarine water. All vertical profiles consisted of 1-m bin averages of the CTD data.

Three profiles during ebb flow (Figure 10a) illustrate the difference in salinity and beam attenuation inside and outside of the plume. The salinity outside the plume was nearly uniform over depth with slight increases near bottom. Inside, the gradient was much greater and showed this section of the plume to be about 6 m deep. Salinities were about 1 psu lower in the plume. Higher beam attenuation was correlated with the lower salinity in the plume. (The occasional increase in beam attenuation at the bottom is probably a result of the CTD hitting the bottom.)

Two hours later, tidal currents were flooding. The salinity deficit in the plume was about 0.5 psu and based on attenuation, the plume was about 4 m deep (Figure 10b). These differences probably result from being about 1 km farther out along the plume front plus de-straining of the density structure.

Time Sections In and Out of the Front

Parameters inside the plume were compared with those outside by plotting vertical profiles versus time (Figure 11). While there is potential for spatial aliasing due to the fact that data in later time were obtained farther out along the plume front, the time sections may approximate what a drifter would pass through as it was advected along the front subject to changing the tidal currents over a 3-hr interval.

Salinity outside the plume was always greater than 32 psu except for a time period about 1 hr after low tide (Figure 11a). Since slack water occurs about 1 hr later than high or low water at the Charleston Harbor entrance (USDC, 1990), this depression in salinity coincided with the approximate time of slack water. It was accompanied by lower temperature and increased beam attenuation (Figure 11b). We must treat this feature in beam attenuation with caution since it is defined by a single station pair, either station of which might be closer into shelf water and/or plume water than the others.

Salinity inside the plume (Figure 11a) showed a halocline deepening from the surface to about 5 m until low tide. Afterwards, the halocline shoaled steadily and was near the

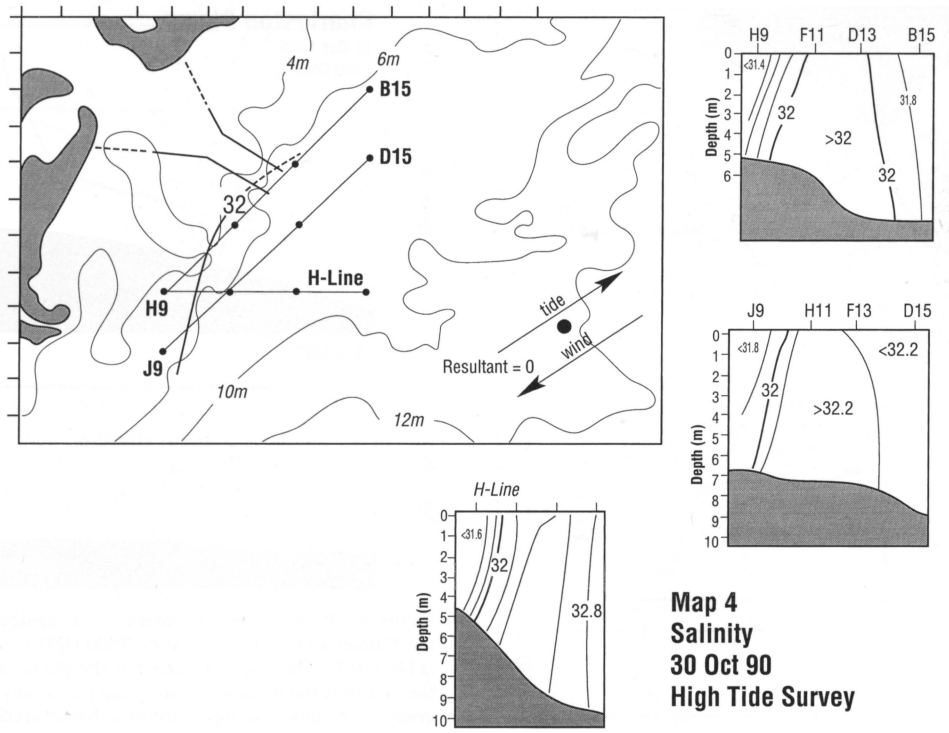

Figure 6. Survey during high water on 30 October 1990 showing surface and vertical salinity sections.

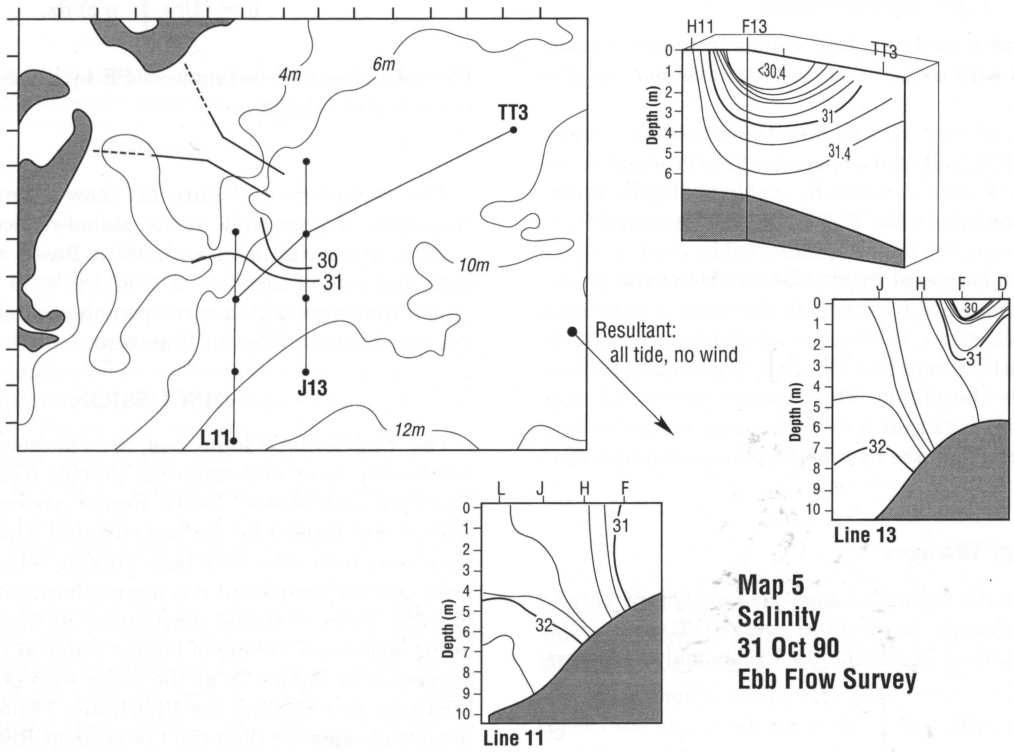

Figure 7. Survey during maximum ebb tide on 31 October 1990 showing surface and vertical salinity sections.

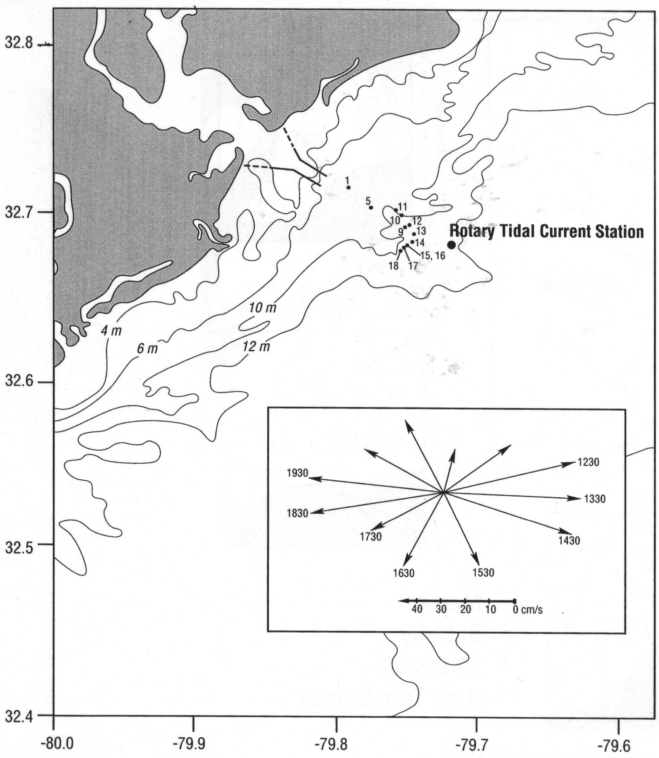

Figure 8. Location map of stations occupied during the dissipation study of 3 October 1990. Also shown is the predicted rotary tidal current at a site 9 km southeast of the inlet to Charleston Harbor (USDC, 1990).

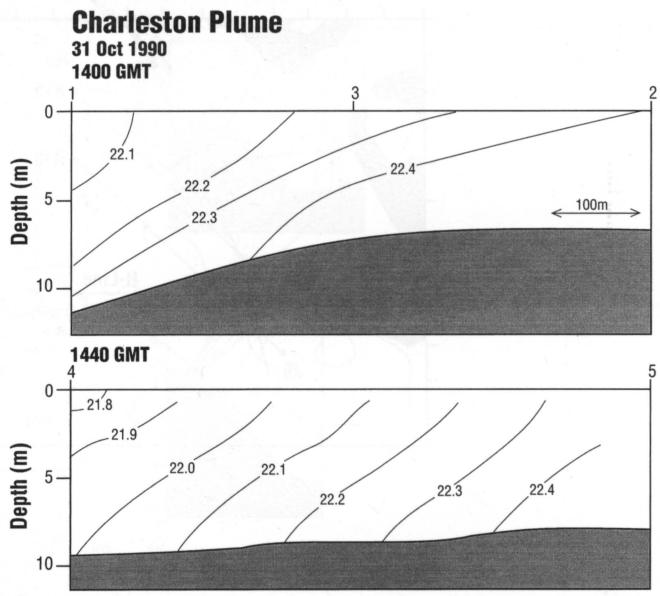

Figure 9. Cross-section of sigma-t on the upstream edge of the Charleston Plume: 2 km from the jetties (1400 GMT) and 4 km from the jetties (1440 GMT). The compact nature of the plume structure is indicated by the fact that the vertical density gradient is only 20 times the horizontal gradient. Numbers at top of sections denote station numbers.

surface about one hour later. Low values in upper level salinity correlated with a maximum in beam attenuation (Figure 11b).

Changes in σ_t (Figure 11c) showed the plume as a region bounded by the 22.2 and 22.6 isopycnals. This gradient weakened at low tide. A zone of neutrally stable or slightly unstable water appeared above the 22.6 isopycnal. The slope of the frontal zone defining the plume is indicated by comparing the depth of the 22.6 isopycnal inside and outside of the plume. The front sloped upward from 6 m to the surface until slack water. After slack water, the horizontal density gradient decreased to essentially zero and all other horizontal gradients weakened across the plume. The unstable region below σ_t values of 22.5 suggests that a reversal occurred in the local pressure gradient below the base of the plume sometime after slack water.

Potential Energy Changes

We summarize the vertical changes in density structure by calculating the changes in potential energy (PE) both inside and outside the plume. We define the PE anomaly as follows:

$$\mathrm{PE} = g \int_0^h (\bar{\rho} - \rho) z \, dz \qquad [1]$$

where z is the vertical coordinate increasing upward with z = 0 at the bottom, h is water depth, ρ is density, g is acceleration due to gravity, and $\bar{\rho}$ is its vertical average density, or

$$\bar{\rho} = (1/h) \int_0^h \rho(z) \, dz.$$

We normalize each estimate of PE by dividing by the depth of the water column or

$$\phi = \mathrm{PE}/h. \qquad [2]$$

The changes in ϕ (Figure 12) show a general increase in the plume. Increased ϕ in the plume reflects a decrease in vertical density gradient over time. Based on linear regression, the rate of increase of ϕ of 1.6×10^{-4} W m^{-3} in the plume compares with a corresponding change in shelf water not significantly different than zero.

DISCUSSION

The Charleston Plume has the characteristics of many small-scale river and estuarine plumes (GARVINE, 1974a,b; GARVINE and MONK, 1974). Fronts associated with these plumes are formed by surface currents which flow into the front from both sides with large sinking velocities. The along-front current component has intense horizontal shear normal to front. There is strong convergence at these fronts that induces *downward* mixing of lighter water at the front. This is suggested in Figure 2b at the outer edge of the plume. The buoyancy flux forming the Charleston Plume is an order of magnitude smaller than the Connecticut River Plume (Table 3; MASSE and MURTHY, 1990). While the Connecticut River Plume was not attached to the bottom, the Charleston Plume

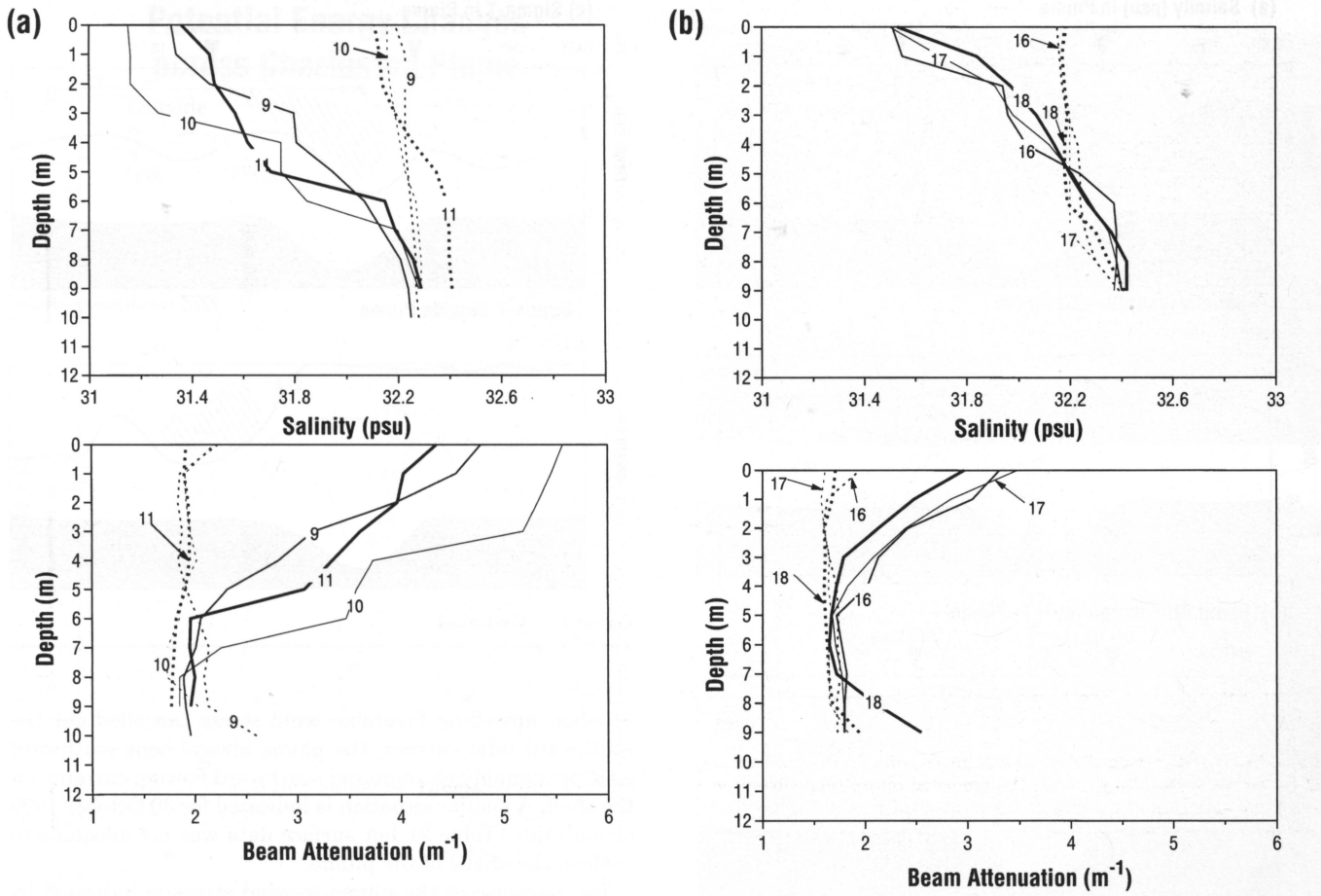

Figure 10. Comparison of vertical profiles of salinity (psu) and beam attenuation (m^{-1}) inside (solid lines) and outside (dashed lines) the plume. (a) Ebb tide; (b) flood tide. Numbers refer to positions marked in Figure 8.

was attached in the shallow water off the jetties (Figure 9) and appeared to lift-off at bottom depths greater than 10 m (Figure 2). The proximity of the bottom in the Charleston Plume may inhibit the downward mixing of lighter water.

The offshore plume boundary off Charleston has a sharp surface front accompanied by a sharp color change marking an abrupt juxtaposition of brown riverine water with blue-green shelf water (Figure 13). No comparative studies were done on the inshore side of the plume where other studies have suggested that the inshore lateral boundary has no sharp front, but rather has an inclined isopycnal structure resulting from more effective mixing in shallower water (GARVINE, 1974b).

Taking all our data as a whole, the Charleston Plume at some tidal phases and at some locations shows evidence of (1) strong tidal current shear flowing mainly along the front; (2) penetration of the ambient shelf water by the estuarine outflow (even during slack water [Figure 3]); and (3) strong convergent flow at the color front. The third constituent is embedded in the other two.

Interaction of Plume with Tidal Currents and Wind

The Charleston Plume exits onto the continental shelf where it interacts with the ambient tidal and wind-generated current. Tidal currents are routinely predicted in the NOAA Tidal Current Tables (USDC, 1990) for a point 9 km southeast of the jetties at the entrance to Charleston Harbor (Figure 8). The predicted rotary current for 31 October 1990 probably represents the tidal current encountered during the other surveys. Maximum flood (ebb) current is about 0.5 m sec^{-1} onshore (offshore); high (low) water slack currents are about 0.2 m sec^{-1} northeast (southwest) (alongshore).

The plume encountered different phases of the rotary tidal current for our surveys. The resultant water motion included the tidal current plus the wind-generated current acting at the time of the survey. During autumn, the average flow on the inner shelf is southward (BLANTON *et al.*, 1994), and we expect the plume to encounter southward alongshore drift except during events of upwelling favorable winds. (Evidence of this response is given below.) These currents are set up in

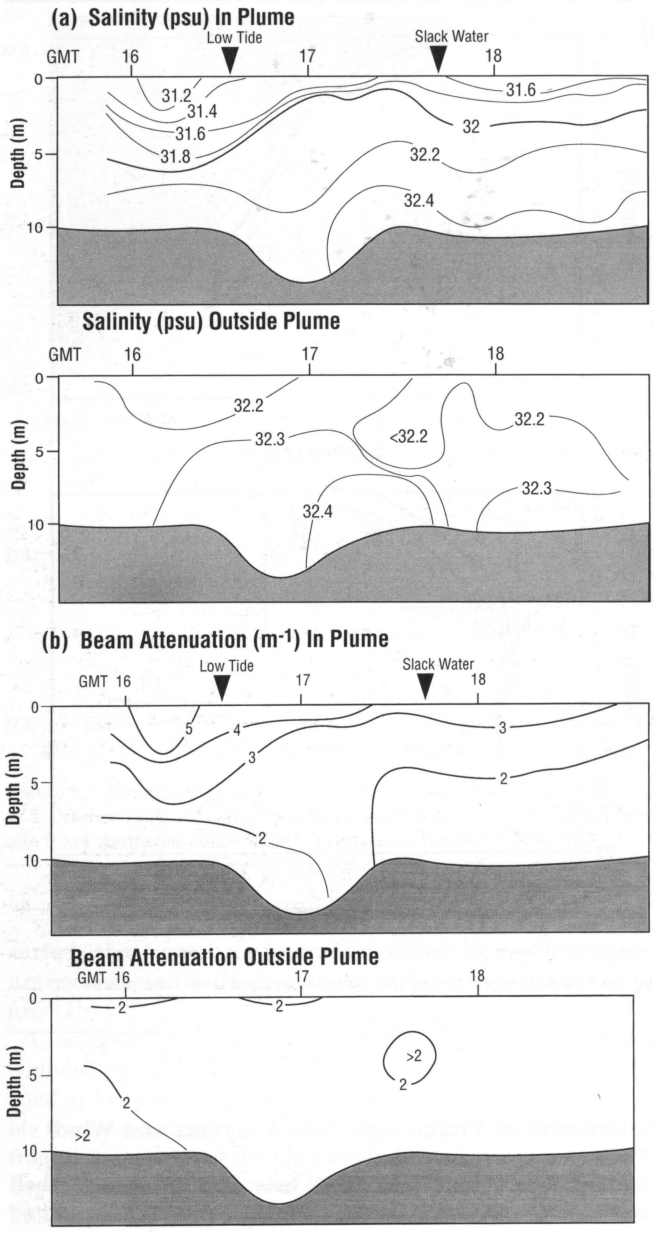

Figure 11. Time series of properties inside and outside the plume. (a) Salinity (psu); (b) beam attenuation (m^{-1}); (c) σ_t (kg m^{-3} − 1000).

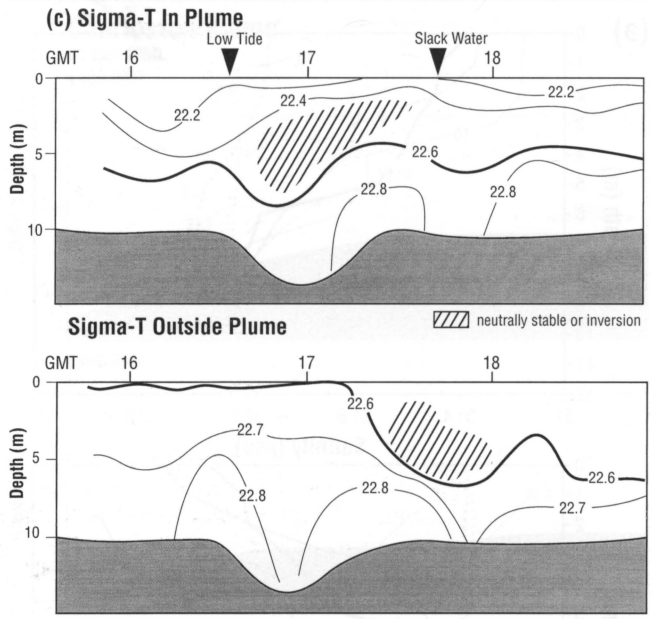

Figure 11. Continued.

about 6 hr (BLANTON *et al.*, 1989a), so we use a simple surface stress/bottom stress momentum balance applicable in the shallow water adjacent to the plume to estimate the magnitude of the wind-generated alongshelf current for each of the surveys (Table 1). We assume that the cross-shelf wind-generated current was negligible. The resultant current is estimated in Table 2.

When taking into account the resultant current as the combined wind drift and tidal currents (Figures 2–7), the measured configuration of the plume conforms to expectation. Except for the slack water survey on 16 November 1991 (Figure 3) when upwelling favorable wind stress cancelled out the southward tidal current, the plume always bent southward as it presumably encountered southward flowing currents on the shelf. A similar situation is indicated for 30 October 1990 at high tide (Table 2), but surface data was not adequate to confirm the shape of the plume.

The response of the plume to wind stress is indicated by aerial photographs of the plume (Figure 13). The plume was clearly bent northward on 17 January 1992 when winds over the region from Savannah, Georgia, to Frying Pan Shoals, North Carolina, were from the south. On 30 October 1990, wind was from the north (Table 2) and the plume bent to the south.

Circulation at the Plume Front

Several features showed up in this study that relate to the circulation of water at the edge of the plume. First, the TSM field at the surface appeared skewed to the left (looking seaward) of the salinity minimum during two of the surveys in 1991 (Figures 2 and 4). Second, neutral or unstable vertical density gradients appeared near the time of slack water. We address these features in this section.

What Causes Instabilities at Slack Water along Plume Front?

The paired CTD station data on either side of the plume indicate zones of neutrally stable or unstable conditions just below the plume at or after the time of slack water. The plume itself decreased in thickness from about 4 m to less than 2 m.

IMBERGER (1983) derived a flow pattern relative to the surface front in which water behind the front moves toward the

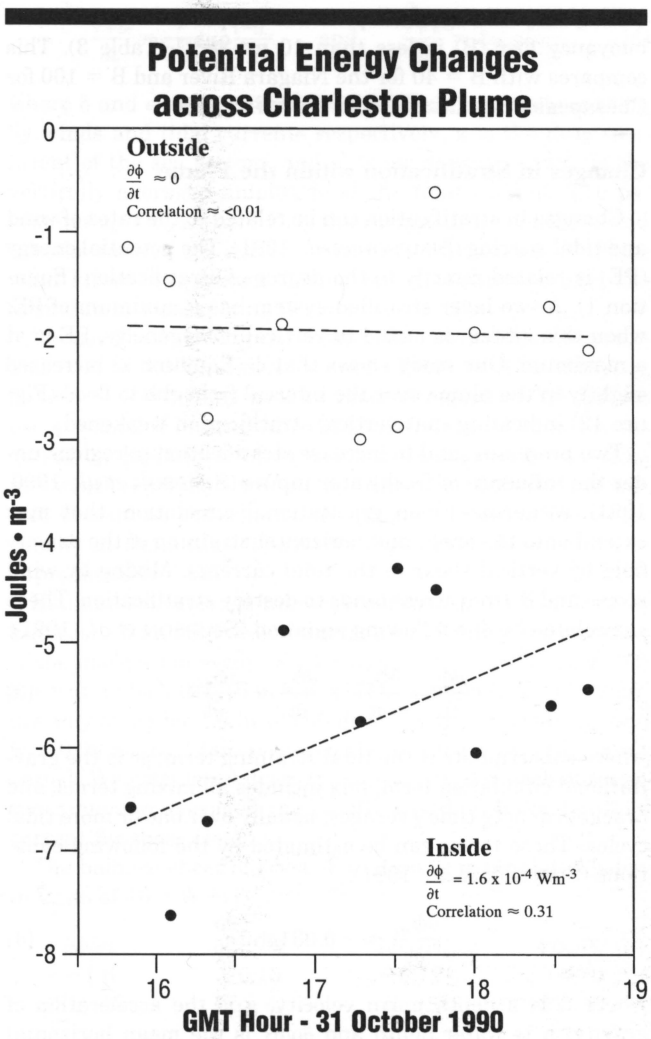

Figure 12. Time series of potential energy changes inside and outside the plume. Dashed lines are $\partial\phi/\partial t$ estimates based on linear regression. See text for details.

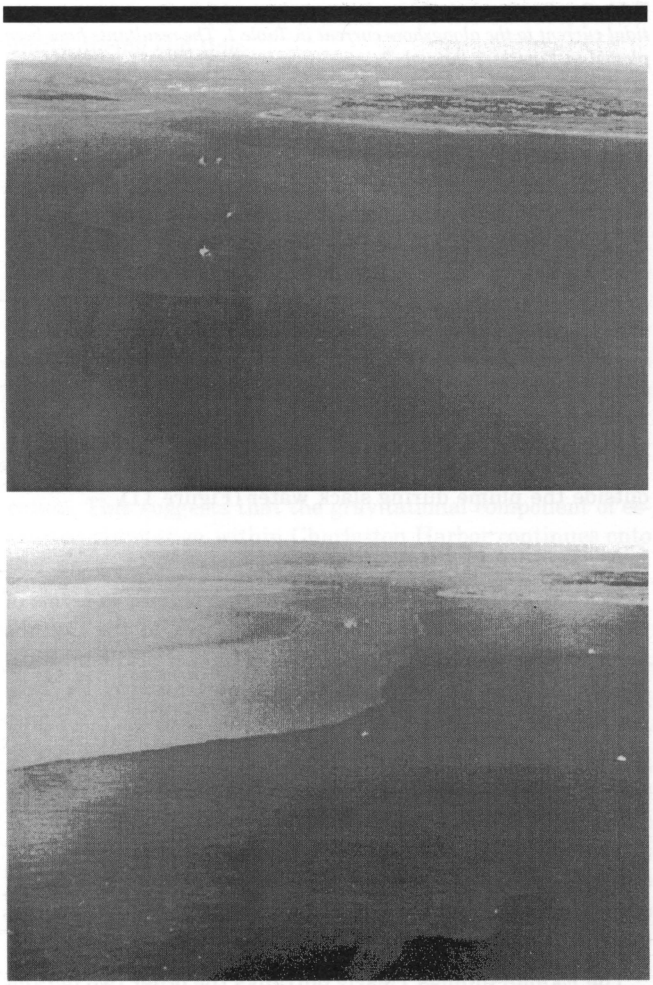

Figure 13. Aerial photographs of the plume. (a) 17 January 1992 with an upwelling favorable wind speed of 14 m sec^{-1}. (b) 2 November 1990 with a downwelling favorable wind speed of 7 m sec^{-1}.

front at the surface, plunges at the front, and returns at depth where it mixes with the ambient underflowing water. Entrainment occurs in the plunging underflow and a "turbulent core" is produced, defined by inflowing plume water at the surface and outflowing (backflowing) mixed ambient and plume water at depth. In the final stages of the front (near low-water slack), the entrainment zone, previously at some depth, rises to the surface and weakens the density differential across the front. With a weakened or nonactive mechanism of entrainment, the inflow depth from the parent plume is considerably reduced which cuts off the pressure gradient force toward the plume's edge and shuts down the turbulent core. Higher density ambient shelf water can now flow underneath the plume (or what remains of it) at a shallower depth. Without an active rotor to pump plume water downward and back underneath the plume, plume water can intrude into shelf water within the neutrally stable region.

Table 1. *Estimate of alongshelf wind-generated current based on alongshelf component of wind stress 6 hours before each plume survey. Local wind data came from the NOAA C-MAN Station (FBISI) at Folly Beach, SC (Figure 1). A quadratic bottom stress coefficient of 0.005 was used for each estimate. Wind stress was calculated according to* BLANTON et al. *1989b).*

Survey Date	Tidal Stage	Alongshore Wind Stress (Pa × 10)	Alongshore Wind-driven Current ms^{-1}
30 Oct 90	Low Water	−0.20	−0.2
30 Oct 90	High Water	−0.15	−0.2
31 Oct 90	Max ebb → Max flood	0	0
16 Nov 91	Low Water	0.37	0.3
17 Nov 91	Max Ebb	−0.80	−0.4
18 Nov 91	Max Flood	−0.86	−0.4

Table 2. *Resultant shelf current ms⁻¹ obtained by vector addition of the tidal current to the alongshore current in Table 1. The resultants have been plotted in Figures 2 through 7.*

Survey Date	Tidal Stage	Wind Current x	Wind Current y	Tidal Current x	Tidal Current y	Resultant Current x	Resultant Current y
30 Oct 90	Low Water	0	−0.2	0	−0.3	0	−0.5
30 Oct 90	High Water	0	−0.2	0	+0.2	0	0
31 Oct 90	Max ebb	0	0	0.5	0	0.5	0
31 Oct 90	Slack	0	0	0	−0.3	0	−0.3
31 Oct 90	Max Flood	0	0	−0.5	0	−0.5	0
16 Nov 91	Low Water	0	0.3	0	−0.3	0	0
17 Nov 91	Max Ebb	0	−0.4	0.5	0	0.5	−0.4
18 Nov 91	Max Flood	0	−0.4	−0.5	0	−0.5	−0.4

This intrusion shows up as a turbid region of reduced salinity outside the plume during slack water (Figure 11).

Classification of Plume

McCLIMANS (1988) classifies estuarine plumes in terms of three dimensionless parameters normalized to the Coriolis parameter: the Rossby number ($\eta = r_i/L$); the rotational Richardson number (r_0^2/Lr_i); and the Ekman number (N_v/D^2f). Here, r_0 is the Rossby radius of deformation $[g'D]^{(1/2)}/f$, where g' is the reduced gravity in the plume, D is the thickness of the plume, and f is the Coriolis parameter; r_i is the inertial circle radius [U/f] where U is the flow speed in the plume; L is a characteristic spreading distance of the plume offshore; and N_v is the vertical eddy viscosity. We use our observations to estimate these and other parameters (Table 3) so that the Charleston plume can be compared with others in terms of the importance of various terms in the equations of motion.

The Ekman number clearly outranks the other two parameters by 1–2 orders of magnitude. With E large and R small, the flow in the plume is controlled largely by vertical friction, with Coriolis force playing a minor if not negligible role. This result is consistent with the observed deflection of the Charleston plume downwind. A Kelvin number (GARVINE, 1987) much less than O(1) also indicates that rotation is negligible. In our case, the Kelvin number is less than O(1) but not significantly so (Table 3).

Buoyancy forcing of the plume is comparatively weak. The buoyancy flux (B) is less than 10 m^4 sec^{-3} (Table 3). This compares with B = 40 for the Niagara River and B = 100 for Chesapeake Bay (MASSE and MURTHY, 1990).

Changes in Stratification within the Plume

Changes in stratification can be related to the rates of wind and tidal stirring (SIMPSON *et al.*, 1991). The potential energy (PE) is related directly to the degree of stratification (Equation 1). A two-layer stratified system has a minimum of PE; when this system is mixed to vertical homogeneity, PE is at a maximum. Our study shows that ϕ (Equation 2) increased slightly in the plume over the interval from ebb to flood (Figure 12) indicating that vertical stratification weakened.

Two processes tend to increase stratification in regions under the influence of freshwater inputs (SIMPSON *et al.*, 1990, 1991): estuarine-driven gravitational circulation, that may extend onto the shelf, and horizontal straining of the density field by vertical shear in the tidal currents. Mixing by wind stress and bottom stress tends to destroy stratification. These are related by the following equation (SIMPSON *et al.*, 1991):

$$\frac{\partial \phi}{\partial t} = \frac{\partial \phi_{str}}{\partial t} + \frac{\partial \phi_{gc}}{\partial t} + \frac{\partial \phi_{mix}}{\partial t} \quad [3]$$

where subscript str is the tidal straining term, gc is the gravitational circulation term, mix includes all mixing terms, and brackets denote time averages, usually over one or more tidal cycles. These terms can be estimated by the following equations (SIMPSON *et al.*, 1991):

$$\frac{\partial \phi_{str}}{\partial t} = -0.031 g h \bar{u} \frac{\partial \rho}{\partial x} \quad [4]$$

where $\bar{u}$ is a depth mean velocity, g is the acceleration of gravity, h is water depth and $\partial\rho/\partial x$ is the mean horizontal density gradient;

$$\frac{\partial \phi_{gc}}{\partial t} = -0.0031 \frac{g^2 h^4}{N_z \rho} \left(\frac{\partial \rho}{\partial x} \right)^2. \quad [5]$$

The mixing term $\partial\phi_{mix}/\partial t$ is comprised of a bottom stress term $\partial\phi_b/\partial t$ and a wind stress term $\partial\phi_w/\partial t$, or

Table 3. *Relevant parameters that scale the Charleston plume to terms in the equation of horizontal motion. Freshwater discharge (Q) into Charleston Harbor is monitored by a power station on the Cooper River.*

Buoyancy flux (m^4 s^{-3})	$B = g'Q$	3
Rossby radius (m)	$r_o = (g'D)^{1/2}/f$	2,300
Intertidal radius (m)	$r_i = U/f$	5,700
Interfacial wave speed (ms^{-1})	$c_i = fr_o$	0.2
Kelvin number	$K = [\text{exit width}/r_o] = [0.7/2.3]$	0.3
Froude number	$Fr = (U^2/c_i^2)$	4
Ekman number	$E = N_V/(fD^2)$	8.9
Rossby number	$\eta = r_i/L = U/fL$	0.6
Rotational Richardson number	$R = (r_o)^2/(Lr_i)$	0.01

The following characteristic values are assumed:

$U = 0.4$ ms^{-1}	$f = 0.7 \times 10^{-4}$ s^{-1}
$L = 10$ km	$g' = (\delta\rho/\rho)g = 0.02$ ms^{-2}
$D = 4$ m	$N_V = 0.01$ m^2 s^{-1}
$H = 10$ m	$Q = 150$ m^3 s^{-1}

$$\frac{\partial \phi_b}{\partial t} = \frac{4}{3\pi}\epsilon\kappa\rho\frac{|\bar{u}_t|^3}{h} \quad \text{and} \quad \frac{\partial \phi_w}{\partial t} = \delta\kappa_s\rho_s\frac{W^3}{h} \qquad [6]$$

where δ and ϵ represent efficiencies of mixing due to stirring by winds and tidal currents respectively, κ is the drag coefficient of the sea bottom, and ρ_s is air density, and $\bar{u}_t$ is the vertically averaged amplitude of the tidal current. The parameter $\kappa_s = C_d\gamma$ where C_d is the surface drag coefficient and γ is the ratio of the surface current to wind speed, W. Since wind stress was absent during our dissipation study, the term due to wind mixing is zero.

We use the following parameters for use in Equations 4, 5 and 6: $\kappa = 0.005$; and $N_z = 0.01$ (Table 3). The efficiency factor $\epsilon = 0.0038$ was used by SIMPSON *et al.* (1991), but we use $\epsilon = 0.02$ (FEARNHEAD, 1975). Estimates of $\partial\rho/\partial x$ are required for Equations 4 and 5. We use a scale of $\delta\rho$ of 1.2 kg m^{-3} which represents the average difference between the surface density at the edge of the plume and estuarine water density at the jetties. The scale length over this distance is approximately 6 km.

Estimates of average tidal current speeds are required for Equations 5 and 6. Predicted tidal currents over the duration of the dissipation study (Figure 8) vary from 0.09 m sec^{-1} at low water slack to 0.16 m sec^{-1} 2.5 hr into flood. Tidal straining only acted for 1.5 hr of ebb flow. For that period, we used $\bar{u} = 0.09$ m sec^{-1} but averaged the result for the 3-hr study period. We calculated discrete values of ϕ_b for each observation time and averaged the results based on predicted tidal current for these times.

The balance sheet of $\partial\phi/\partial t$ (Equation 3) is tabulated below in units of 10^{-4} W m^{-3}.

$\partial\phi/\partial t$	$\partial\phi_{str}/\partial t$	$\partial\phi_{gc}/\partial t$	$\partial\phi_b/\partial t$
+1.6	−0.13	−0.12	+0.20
(Fig. 12)	(Eq. 4)	(Eq. 5)	(Eq. 6)

This model requires good estimates of current profiles and horizontal density gradients. Current profile measurements were not available for this study, so there is a wide margin through which to adjust values of $\bar{u}_t$ and N_z. Moreover, the estimate of $\partial\phi/\partial t$ in the plume is based on a linear regression analysis of data with considerable noise.

The above result suggests that vertical mixing has been significantly underestimated. Over a complete tidal cycle during which the RMS amplitude of depth average currents is about 0.25 m sec^{-1}, $\partial\phi_b/\partial t$ is $O(10^{-5})$ W m^{-3}, or $O(10^{-4})$ W m^{-3}, depending upon the value of ϵ. On the other hand, ϕ_{gc} and ϕ_{str} depend upon $\partial\rho/\partial x$ which was estimated to be particularly large on the upstream edge. A more "global" value for the time span of the experiment would probably be lower. Therefore, we must question how representative are our ϕ estimates along a single edge of the plume.

It is clear that $\partial\phi_t/\partial t$ of order 10^{-4} W m^{-3} is required to overcome the stratifying tendency of tidal straining and gravitational circulation. Uncertainty in the appropriate value of ϵ renders any estimate debatable. In the waning portion of the ebb cycle and beginning of flood, vertical mixing via bottom stress appears to be negligible, but interfacial stresses may provide a significant portion of the required stress. These undoubtedly occur along the plume edge where Kelvin-Hemholtz instabilities are prominent at the surface, particularly during ebb tide.

CONCLUSIONS

The Charleston Plume is bottom attached. It is influenced by wind and tidal currents and is easily deflected by the alongshelf wind stress. These findings are consistent with the classification of estuarine plumes by MCCLIMANS (1988). A simple stratification model (SIMPSON *et al.*, 1991) was used to assess the energetics associated with observed density gradients. The change in ϕ observed in the plume was partially offset by tidal straining, gravitational circulation. Dissipation by bottom stress was apparently too low to account for the total observed changes in ϕ. Despite the relatively weak buoyancy flux, gravitational circulation and tidal straining appears to be important in maintaining the vertical stratification. This suggests that the gravitational component of estuarine circulation within Charleston Harbor continues onto the continental shelf.

ACKNOWLEDGEMENTS

We are grateful for the excellent and professional help of Captain James Gault and Jay Fripp aboard the R/V BLUE FIN and also gratefully acknowledge the help of Peter Verity and Craig Tronzo of Skidaway Institute of Oceanography in support of collecting the data for this project. Charles A. Barans of South Carolina Marine Resources Research Institute kindly provided the photos for Figure 13. We also thank Bjorn Kjerfve and Amo Oliveira of the University of South Carolina for providing oceanographic data on the plume during the 1990 surveys. This paper is funded by the National Oceanographic and Atmospheric Administration Coastal Ocean Program Office through Grant NA36RG0398 to the Georgia Sea Grant Program and by Grant NA26RG-0-37301 to Skidaway Institute of Oceanography from the Georgia Sea Grant Program.

LITERATURE CITED

VAN AKEN, H.M., 1986. The onset of seasonal stratification in shelf areas due to differential advection in the presence of a salinity gradient. *Continental Shelf Research,* 5, 475–485.

ATKINSON, L.P. and BLANTON, J.O., 1986. Processes that affect stratification in shelf waters. Baroclinic Processes on Continental Shelves. *Coastal Estuarine Science,* Vol. 3, Washington, D.C.: AGU, pp. 117–130.

BAILEY, A.C., 1988. Solute and Particle Gradients in the Benthic Boundary Layer. Ph.D. Dissertation, Clemson, South Carolina: Clemson University, Department of Chemistry, 142p.

BLANTON, J.O. Reinforcement of gravitational circulation by wind. *In: Seventh Biennial Conference on Physics of Estuaries and Coastal Seas.* In press.

BLANTON, J.O., 1981. Ocean currents along a nearshore frontal zone on the continental shelf of the southeastern United States. *Journal of Physical Oceanography,* 11(12), 1627–1637.

BLANTON, J.O.; AMFT, J.A.; LEE, D.K., and RIORDAN, A., 1989a. Wind stress and heat fluxes observed during Winter and Spring, 1986. *Journal of Geophysical Research,* 94, 10686–10698.

BLANTON, J.O. and ATKINSON, L.P., 1983. Transport and fate of river discharge on the continental shelf of the southeastern United States. *Journal of Geophysical Research,* 88, 4730–4738.

BLANTON, J.O.; OEY, L.-Y.; AMFT, J., and LEE, T.N., 1989b. Advec-

tion of momentum and buoyancy in a coastal frontal zone. *Journal of Physical Oceanography,* 19, 98–115.

BLANTON, J.; WERNER, F.; KIM, C.; ATKINSON, L.; LEE, T., and SAVIDGE, D., 1994. Transport and fate of low-density water in a coastal frontal zone. *Continental Shelf Research,* 14, 401–427.

FEARNHEAD, P.G., 1975. On the formation of fronts by tidal mixing around the British Isles. *Deep-Sea Research,* 22, 311–321.

GARVINE, R.W., 1974a. Dynamics of small-scale oceanic fronts. *Journal of Physical Oceanography,* 4, 557–569.

GARVINE, R.W., 1974b. Physical features of the Connecticut River outflow during high discharge. *Journal of Geophysical Research,* 79, 831–846.

GARVINE, R.W. and MONK, J.D., 1974. Frontal structure of a river plume. *Journal of Geophysical Research,* 79, 2251–2259.

GARVINE, R.W., 1987. Estuary plumes and fronts in shelf waters: A layer model. *Journal of Physical Oceanography,* 17, 1877–1896.

GARVINE, R.W., 1991. Subtidal frequency estuary-shelf interaction: Observations near Delaware Bay. *Journal of Geophysical Research,* 96, 7049–7064.

HEARN, C.J.; HUNTER, J.R.; IMBERGER, J., and VAN SENDEN, D., 1985. Tidally induced jet in Koombana Bay, Western Australia. *Australian Journal of Marine Freshwater Research,* 36, 453–479.

IMBERGER, J., 1983. Tidal jet frontogenesis. Transactions of the Institution of Engineers. *Mechanical Engineering,* 8, 171–180.

JIRKA, G.H., ADAMS, E.E., and STOLZENBACH, K.D., 1981. Buoyant surface jets. *American Society of Civil Engineers Journal of Hydraulics Division,* 107(HY11), 1467–1487.

JOHANNESSEN, J.A.; SVENDSEN, E.; SANDVEN, S.; JOHANNESSEN, O.M., and LYGRE, K., 1989. Three-dimensional structure of mesoscale eddies in the Norwegian coastal current. *Journal of Physical Oceanography,* 19, 3–19.

MASSE, A.K., 1990. Withdrawal of shelf water into an estuary: A barotropic model. *Journal of Geophysical Research,* 95, 16085–16096.

MASSE, A.K. and MURTHY, C.R., 1990. Observations of the Niagara River thermal plume (Lake Ontario, North America). *Journal of Geophysical Research,* 95, 16097–16109.

MASSE, A.K. and MURTHY, C.R., 1992. Analysis of the Niagara plume dynamics. *Journal of Geophysical Research,* 97, 2403–2420.

MCCLIMANS, T.A., 1988. Estuarine fronts and river plumes. *In*: DRONKERS, J. and VAN LEUSSEN, W. (eds.), *Physical Processes in Estuaries.* Berlin: Springer-Verlag, pp. 55–69.

MORK, M., 1981. Circulation phenomena and frontal dynamics of the Norwegian coastal current. *Philosophical Transactions of the Royal Society of London A,* 302, 635–647.

PAPE III, E.H. and GARVINE, R.W., 1982. The subtidal circulation in Delaware Bay and adjacent shelf waters. *Journal of Geophysical Research,* 87(C10), 7955–7970.

PIETRAFESA, L.J.; BLANTON, J.O.; WANG, J.D.; KOURAFALOU, V.; LEE, T.N., and BUSH, K.A., 1985. The tidal regime in the south Atlantic Bight. *In*: ATKINSON, L.P.; MENZEL, D.W., and BUSH, K.A. (eds.), *Oceanography of the Southeastern United States Continental Shelf.* Washington, D.C.: AGU, pp. 63–76.

ROYER, T.C., 1981. Baroclinic transport in the Gulf of Alaska, Part II. A fresh water driven coastal current. *Journal of Marine Research,* 39, 251–266.

SAFAIE, B., 1978. Mixing of horizontal buoyant surface jet over a sloping bottom. *Hydraulic Engineering Laboratory Report HEL 27-4,* Berkeley: University of California, 198p.

SIMPSON, J.H. and HILL, A.E., 1986. The Scottish coastal current. *In*: SKRESLET, S. (ed.), *The Role of Freshwater Outflow In Coastal Marine Ecosystems,* Vol. I, *NATO Advance Study Inst. Series, Ser G,* pp. 295–308.

SIMPSON, J.H.; BROWN, J.; MATTHEWS, J., and ALLEN, G., 1990. Tidal straining, density currents and stirring in the control of estuarine stratification. *Estuaries,* 13, 125–132.

SIMPSON, J.H.; SHARPLES, J., and RIPPETH, T., 1991. A prescriptive model of stratification induced by freshwater runoff. *Estuarine and Coastal Shelf Science,* 33, 23–35.

U.S. DEPARTMENT OF COMMERCE, 1990. *Tidal Current Tables 1990: Atlantic Coast of North America.* Washington, D.C.: NOAA, 243p.

U.S. ENVIRONMENTAL PROTECTION AGENCY, 1979. *Methods for Chemical Analysis of Water and Wastes.* EPA-600/4-79-020.